Accepted Manuscript

Serum Albumin's Protective Inhibition of Amyloid-β Fibre Formation Is Suppressed by Cholesterol, Fatty Acids and Warfarin

David C. Bode, Helen F. Stanyon, Trisha Hirani, Mark D. Baker, Jon Nield, John H. Viles

PII: S0022-2836(18)30021-4
DOI: https://doi.org/10.1016/j.jmb.2018.01.008
Reference: YJMBI 65590

To appear in:

Received date: 24 October 2017
Revised date: 10 January 2018
Accepted date: 12 January 2018

Please cite this article as: David C. Bode, Helen F. Stanyon, Trisha Hirani, Mark D. Baker, Jon Nield, John H. Viles , Serum Albumin's Protective Inhibition of Amyloid-β Fibre Formation Is Suppressed by Cholesterol, Fatty Acids and Warfarin. The address for the corresponding author was captured as affiliation for all authors. Please check if appropriate. Yjmbi(2018), https://doi.org/10.1016/j.jmb.2018.01.008

For submission to: **JMB revised**

Serum Albumin's Protective Inhibition of Amyloid-β Fibre Formation is Suppressed by Cholesterol, Fatty Acids and Warfarin

David C. Bode[1]*, Helen F. Stanyon[1]*, Trisha Hirani[1]*, Mark D. Baker[2], Jon Nield[1], John H. Viles[1]

[1]School of Biological and Chemical Sciences, Queen Mary University of London, Mile End Rd., London E1 4NS, UK

[2] Blizard Institute, Queen Mary University of London, Whitechapel E1 2AT

Running title: **Serum albumin and amyloid-β fibre formation**

*Have contributed equally

To whom correspondence should be addressed: John H. Viles, E-mail: j.viles@qmul.ac.uk

Keywords: Alzheimer's disease; Aβ; HSA; ion channels; oligomers;

Abbreviations: Amyloid-β peptide, Aβ ; Analysis of Variance ANOVA; Alzheimer's Disease, AD; Cerebral Spinal Fluid, CSF; Central Nervous System, CNS; Genome wide association study, GWAS; Human Serum Albumin, HSA; Interstitial fluid, ISF; Transmission electron microscope, TEM.

ABSTRACT

Central to Alzheimer's disease (AD) pathology is the assembly of monomeric amyloid-β peptide (Aβ) into oligomers and fibres. The most abundant protein in the blood plasma and cerebrospinal fluid (CSF) is human serum albumin (HSA). Albumin can bind to Aβ and is capable of inhibiting the fibrillisation of Aβ at physiological (μM) concentrations. The ability of albumin to bind Aβ has recently been exploited in a phase-II clinical trial, which showed a reduction in cognitive decline in Alzheimer's disease patients undergoing albumin plasma-exchange. Here we explore the equilibrium between Aβ monomer, oligomer and fibre in the presence of albumin. Using transmission electron microscopy and thioflavin-T fluorescent dye, we have shown albumin traps Aβ as oligomers, 9 nm in diameter. We show that albumin-trapped Aβ oligomeric assemblies are not capable of forming ion-channels, which suggests a mechanism by which albumin is protective in Aβ exposed neuronal cells. *In vivo* albumin binds a variety of endogenous and therapeutic exogenous hydrophobic molecules, including cholesterol, fatty acids, and warfarin. We show these molecules bind to albumin and suppress its ability to inhibit Aβ fibre formation. The interplay between Aβ, albumin and endogenous hydrophobic molecules impacts Aβ assembly; thus changes in cholesterol and fatty acid levels *in vivo* may impact Aβ fibrillisation, by altering the capacity of albumin to bind Aβ. These observations are particularly intriguing given that high cholesterol or fatty acid diets are well established risk-factors for late-onset AD.

INTRODUCTION

Alzheimer's disease (AD) is the main cause of dementia and affects 47 million people worldwide [1]. A range of evidence points to a small 39-43 residue peptide, Amyloid-β (Aβ), that self-assembles into cytotoxic oligomers and fibres that are thought to be essential contributors to the cascade of events in AD aetiology [2]. Aβ(1-40) and Aβ(1-42) are the most abundant isoforms in the brain interstitial fluid/cerebrospinal fluid (ISF/CSF) and in plaques. In particular, Aβ(1-42) is thought to disrupt cellular ionic homeostasis through the insertion of oligomeric Aβ assemblies into the cellular membrane, leading to the formation of ion channel pores which span the lipid bilayer [3].

There are numerous endogenous proteins and metal ions that interact with Aβ and influence its assembly process both *in vitro* and in animal models [4-8]. Human serum albumin (HSA) is one such protein able to inhibit fibre formation at physiological concentrations [9]. Furthermore, reduced serum HSA levels are correlated with cognitive impairment in AD patients [10, 11] and the elderly[12]. Albumin is the most abundant extracellular protein in blood plasma, at a concentration of 640 μM [13]. It has been shown that albumin binds 90-95 % of the Aβ found in blood plasma [14, 15]. The ability of albumin to sequester Aβ explains why Aβ fibre deposits are not observed in the peripheral vasculature, even though Aβ is found in the blood plasma at 0.1 to 0.5 nM concentrations, at comparable levels to within the cerebrospinal fluid (CSF) [16, 17]. Albumin, which is derived from vascular leakage across the blood-brain-barrier, is also the most abundant protein in the ISF/CSF at 3 μM [18].

In vitro HSA is known to inhibit both Aβ(1-40) and Aβ(1-42) fibrillisation [9, 19-21]. Aβ can interact with hydrophobic binding pockets within all three domains of HSA with similar affinities[22 23]. Albumin can also reduce the cytotoxicity of Aβ(1-42) in SH-SY5Y cell viability assays and primary cell culture [19, 24], which suggests a reduction of toxic oligomers, as well as fibres. We have previously shown that even micromolar ISF/CSF concentrations of HSA inhibit Aβ fibre formation, decreasing both the rate at which fibres form and the total amount of fibres produced [9]. Thus the presence of albumin in blood plasma, but also the brain interstitium, can potentially directly impact Aβ assembly.

One quarter of Aβ is cleared from the brain interstitium by transport across the blood-brain barrier into blood serum [25]. Aβ traffics between CSF/ISF and blood [26-29], and albumin is

important in this clearance by acting as a sink for Aβ in blood serum [30]. Indeed a decrease in blood serum levels of Aβ-albumin complexes is observed in AD [10, 11]. In an AD 3xTg mice model, infusion of HSA intracerebroventricularly caused a reduction in Aβ(1-42) soluble oligomers and total plaque area [31]. The use of albumin as a therapeutic approach, in sequestration of Aβ via plasma exchange, has been explored [32-36] and is receiving a good deal of interest [37]. Recent phase-II clinical trials using an albumin Aβ plasma-exchange approach have shown some improvements in cognition using the Boston Naming Test and a Semantic Verbal Fluency Test [36].

Albumin is capable of transporting many different hydrophobic molecules within blood plasma [13]; including cholesterol [38, 39], fatty acids, such as palmitic acid [40, 41], as well as a number of hydrophobic therapeutic molecules, for example warfarin [42]. We postulated that these endogenous and exogenous hydrophobic molecules might compete with Aβ for the binding of albumin, and so might influence Aβ assembly in the presence of HSA. These molecules are particularly interesting owing to high dietary levels of fatty acids and cholesterol, increasing the risk of developing dementia and AD [43-48]. Furthermore, genome-wide association studies (GWAS) point to cholesterol metabolism as a key AD risk factor [49, 50] and an increase in cholesterol within the central nervous system (CNS) is observed both in the aging and in early AD patients [51]. In agreement with Alzheimer's pathology, AD phenotypes in animal models are exacerbated by elevated dietary cholesterol [52-54], however the mechanism by which cholesterol accelerates disease progression has not yet been established [55].

Aβ fibres exist in a dynamic equilibrium with Aβ monomer, where fibres represent a thermodynamically stable species in the Aβ assembly folding landscape. In this study, we have used ThT fluorescence and transmission electron microscopy (TEM) to follow Aβ fibre growth and disassembly, in the presence of HSA, over different stages of the assembly pathway, in order to gain a more thorough understanding of how albumin impacts the equilibrium between Aβ monomer, oligomer and fibre. Our TEM data suggests HSA traps Aβ in an oligomeric form, and we have characterised the size of the trapped oligomers and investigated their ability to form harmful ion channels in cell membranes. Furthermore, we show that HSA bound ligands, cholesterol, fatty acids and warfarin, disrupt the Aβ-HSA interaction and suppress the inhibitory effect of HSA on Aβ fibrillisation. We suggest that this has significant ramifications for the role of HSA in the inhibition of Aβ fibre formation in the brain interstitium.

RESULTS

Albumin traps Aβ as Oligomers and Inhibits Fibre Growth

We sought to understand how albumin can influence the different stages of Aβ assembly, and how albumin can impact the equilibrium between Aβ monomer, oligomer and fibre. In the absence of HSA, Aβ exhibits a characteristic fibre growth with an initial lag phase during nucleation followed by rapid elongation to form fibres. We have previously shown HSA is able to markedly retard Aβ fibrillisation when added to monomeric Aβ [9]. We wanted to determine if albumin could inhibit fibre formation when substantial amounts of oligomers and curvy-linear Aβ protofibrils were permitted to form before albumin was added to the assembling Aβ solution. We monitored Aβ fibre growth using ThT, a fluorophore that selectively binds to amyloid fibres and produces an intense fluorescence, while monomeric and oligomeric Aβ produces minimal ThT fluorescence [56]. Monomeric Aβ(1-40) was incubated in a 96-well-plate and the ThT fluorescence signal monitored. Albumin was then added to half of the wells containing Aβ solution towards the end the lag-phase, just before rapid elongation of fibres occurred. Even though appreciable amounts of nucleating Aβ oligomers and protofibrils were found to be present, the addition of albumin completely inhibited further assembly of Aβ into fibres, as shown in Figure 1. This data indicates albumin can halt the further assembly of Aβ oligomers into fibres by inhibiting monomer addition of otherwise elongating fibres.

We have also probed the impact of albumin on Aβ assembly using TEM. Figure 2 compares the effect of Aβ assembly in the absence and presence of HSA. Our TEM images clearly show that monomeric Aβ(1-40) and Aβ(1-42) incubated in the presence of 50 μM HSA, are only capable of assembling into a large quantity of small circular oligomers while fibre formation is inhibited, Figure 2d,f. These Aβ assemblies in the presence of albumin are relatively small, perhaps explaining why they have not previously been reported. The TEM images of control albumin appear very different, the 66 kDa albumin molecule being barely observable, appearing as speckles throughout the grid, Figure 2c. Albumin (50 μM) was also added to Aβ (10 μM) at the end of the lag-phase of Aβ assembly (as in Figure 1) and incubated with HSA for 2 days. In agreement with the ThT measurements, TEM micrographs here indicate Aβ as being trapped at the oligomeric stage with a very limited number of mature fibres also observed, Figure 2e.

Albumin trapped Aβ(1-40) and Aβ(1-42) oligomers were surveyed further using single particle analysis of negatively stained images. A dataset of 368 and 206 oligomers were used for each Aβ isoforms, respectively. The data highlights the relatively homogeneous nature of the oligomer assembles with a limited range of diameters and morphologies. Representative class averages are shown for both Aβ(1-40) and Aβ(1-42) indicating the range of oligomers observed, as shown in Figure 3. The approximately spherical oligomers were calculated to have an average diameter of 9 +/- 1 nm, suggesting a molecular mass of approximately 270 kDa; across a range of 190-360 kDa. It is clear that HSA traps Aβ assembly at an early stage of oligomerization. Smaller oligomers might also be present but of comparable in size to albumin.

As fibres are thermodynamically very stable, we wondered whether Aβ would eventually form fibres even in the presence of HSA if given sufficient time, so we chose to monitor potential fibre formation using ThT fluorescence over a number of weeks. Figure 4 presents ThT fluorescence data for the fibrillisation of 10 μM Aβ(1-40) in the absence and presence of 20 μM HSA, over a period of 38 days. In the absence of albumin, a fluorescent peak centred at 485 nm was visible within the first few hours of incubation, indicating ThT bound to Aβ fibres. The maximum ThT fluorescence at 485 nm, as a function of time, is shown in Figure 4c. It is apparent from Figure 4, that Aβ fibrillisation was completely inhibited in the presence of 20 μM HSA and did not show any signs of appearing even after 38 days. HSA has a weak affinity for ThT [57], and does not compete for ThT binding to fibres (shown later in Figure 5), thus the lack of ThT fluorescence in the presence of HSA is attributable to the inhibition of fibre formation, as confirmed by the TEM studies. ThT binds to the hydrophobic pockets in HSA and fluoresces weakly [57], but this fluorescence is negligible compared to ThT when bound to fibres.

In the absence of albumin the ThT fluorescence signal of Aβ fibres was reduced by a third after 38 days, Figure 4c. This reduction in ThT intensity could be due to the very slow lateral association of fibres into larger bundles, conceivably displacing ThT from the surface of fibres. A similar reduction in ThT signal caused by lateral association of N-terminally truncated Aβ(11-40) fibres has recently been reported [58].

Disassembly of pre-formed Aβ fibres does not occur or is too slow to be observed

We also wished to investigate the reverse reaction of albumin addition to preformed fibres. We hypothesised that given sufficient time, albumin might be able to disassemble the fibres. If HSA binds non-fibrillar Aβ species, then over time albumin should be able to solubilise mature Aβ fibres to monomers/oligomers. We monitored the ThT fluorescence of pre-formed Aβ fibres (10 μM Aβ monomer equivalent) in the presence of 0, 3, 20 and 200 μM HSA for 22 days, with ThT fluorescence plotted as a function of time, as shown in Figure 5. In the presence of HSA, the ThT signal for Aβ fibres remained intense over a 22-day period. The ThT signal stayed constant for Aβ fibres in the presence of 3, 20 and even 200 μM albumin, suggesting HSA was unable to disassemble Aβ fibres over a period of three weeks. TEM was also used to investigate the impact of albumin on preformed fibres. In agreement with the ThT studies, Figure 2h shows that the addition of 50 μM albumin to preformed fibres does not impact the quantity of preformed Aβ fibres.

We were concerned that albumin might bind to ThT and generate its own fluorescence signal, however from Figure 5, ThT fluorescence for each for the different HSA concentration did not vary markedly. This confirmed the contribution of ThT fluorescence owed to weak HSA binding was negligible compared to that from ThT bound to fibres. The ThT fluorescence for Aβ with no HSA present was observed to decline a little from a maximum intensity of 340 AFU to 210 AFU after 9 days, a similar loss of ThT signal is also shown in Figure 4c. Interestingly, HSA can stop the gradual loss in ThT fluorescence signal, perhaps by preventing lateral association of the preformed fibres.

Cholesterol and Fatty Acid Loaded HSA Supresses Albumin's Inhibition of Aβ Fibrillisation

Cholesterol is a known risk factor for developing AD [45, 47, 59] and is also known to bind albumin [38, 39]. We wanted to investigate the effect of cholesterol-loaded HSA on Aβ fibrillisation kinetics to determine if cholesterol bound to albumin may influence albumin's ability to supress Aβ fibre formation. Figure 6 shows the kinetic traces of ThT binding to fibres, obtained for Aβ in the presence and absence of albumin and cholesterol-loaded albumin. It is evident that 20 μM albumin will completely inhibit fibrillisation of 10 μM Aβ(1-40), Figure 6b. However, albumin loaded with an equimolar concentration (1:1) of cholesterol no longer inhibits fibre growth, and fibrillisation is largely recovered, Figure 6c. The ThT signal is

almost as intense as that for Aβ in the absence of albumin. TEM images of Aβ(1-40) incubated with cholesterol bound albumin confirms Aβ is able to form amyloid fibres similar in appearance to those formed in the absence of albumin, Figure 6d.

The effect of sub- and supra-stoichiometric amounts of cholesterol loaded albumin (30 μM) on fibre formation was also studied, shown in supplemental figure S1. It is clear 1:1 stoichiometry's and above almost completely negates albumins protective effects on fibre formation, although with delayed lag-times. Interestingly, just one-sixth of a molar-equivalent of cholesterol (30 μM albumin + 5 μM cholesterol) is sufficient to cause considerable recovery of the Aβ fibre growth, as shown in supplemental figure S1c. The observation that sub-stoichiometric amounts of cholesterol can cause the ThT signal to almost completely recover suggest that cholesterol can exchange between albumin molecules. An alternative explanation could involve the association of cholesterol with Aβ which permits fibres to form but inhibits Aβs interaction with albumin. It is notable cholesterol alone does not impact total Aβ fibre load, as shown in supplemental Figure S2. In addition, the presence of 2 % DMSO (v/v) used to solubilise cholesterol does not affect the fibre formation, also shown in Figure 6a.

The concentration of albumin in CSF is approximately 3 μM, so we also studied the effect of this lower concentration of albumin on Aβ(1–40) fibrillisation, supplemental Figure S3. This lower concentration of HSA does not completely inhibit fibril formation but caused an increase in the lag-time (t_{lag}), a decrease in the apparent rate of elongation (k_{app}) and a reduction in total ThT signal, as we have previously reported [9]. The cholesterol-loaded HSA partially returned fibre growth to that of Aβ in the absence of albumin. In particular, the apparent elongation rate (k_{app}), the t_{50} and the total amount of ThT fluorescence was closer to that of Aβ in the absence of albumin. This indicates that equimolar cholesterol bound to HSA can suppress the inhibitory action on Aβ(1-40) fibre formation at concentrations found in the CSF. Despite cholesterol's modest affinity for albumin [38, 60], it is clear that cholesterol will strongly compete with Aβ for albumin binding, and this was indeed the case at 3, 10 and 20 μM albumin concentrations.

Albumin is a transport protein for fatty acids and the binding of as many as seven palmitic acid molecules have been characterised within albumin [41]. The effect albumin has on Aβ(1–40) fibrillisation when loaded with 7 molar equivalents of palmitic acid is shown in Figure 7. When the HSA (10 μM) was loaded with palmitic acid, the Aβ fibre growth was no longer inhibited by the fatty acid loaded albumin, and returned to its maximum ThT

fluorescence, Figure 7c. Similar experiments with 20 μM albumin produced similar behaviour, supplemental Figure S4.

Warfarin Negates the Inhibitory Effect that Albumin has on Aβ Fibrillisation.

Albumin has a number of hydrophobic pockets and as a consequence it is able to bind to a range of exogenous hydrophobic therapeutic molecules, with warfarin being one such molecule [42]. Warfarin is an anti-coagulant prescribed to individuals with a risk of forming blood clots and stroke, such as those with heart arrhythmia. As much as 99 % warfarin in blood plasma is bound to HSA [42]. With this in mind, we monitored Aβ fibre growth in the presence and absence of warfarin bound to albumin. The ThT fluorescence fibre growth curves in the presence and absence of warfarin bound albumin are shown in Figure 8. As previously shown, Aβ incubated in the presence of 30 μM HSA generated no detectable fibres (Figure 8b). In contrast, in the presence of HSA loaded with warfarin (4 molar-equivalent) Aβ is now able to form fibres (Figure 8c) to the same extent as to when albumin is absent. The ThT signal is comparable to that for Aβ alone. A one-way analysis of variance (ANOVA) with Tukey-HSD post-hoc tests revealed no significant difference in maximum fluorescence intensity between Aβ alone and Aβ incubated with 30 μM warfarin-loaded albumin. TEM confirms the formation of amyloid fibres, Figure 8d, in the presence of warfarin loaded albumin.

A control experiment shows that Warfarin alone does not interfere with Aβ fibrillisation. Indeed there was no significant difference in maximum fluorescence or rate of fibre formation (t_{50}, t_{lag} and k_{app}) between Aβ alone and Aβ in the presence of warfarin, see supplemental Figure S5.

Next we investigated the effect of sub-stoichiometric warfarin (15 μM warfarin and 30 μM albumin). Sub-stoichiometric amounts of warfarin are sufficient to cause the return of Aβ fibre formation, although there is a marked delay in the rate of fibre formation, and the maximum intensity of the ThT signal completely returns, supplemental Figure S6.

HSA-trapped Aβ oligomers are incapable of forming ion channels in cellular membranes

The assembly state of Aβ is critical in exerting synaptic dysfunction and cytotoxicity. Oligomeric preparations which are otherwise indistinguishable by size can have starkly different abilities to exert cellular toxicity. Aβ(1-42) ion channel formation is a mechanism by which Aβ is thought to be synaptotoxic. We therefore wanted to determine if the albumin

trapped Aβ(1-42) oligomers are capable of forming ion channel pores in cellular membranes. Here, patches of cell membrane were excised from HEK293 cells. Aβ samples at 5 μM were then delivered to the extracellular face of the membrane within a glass pipette, and transmembrane currents were measured by clamping the patch at a series of step voltage potentials. Preparations of Aβ(1-42) oligomer formed in both the presence and absence of HSA were studied, with between 18 and 49 patches of cellular membrane excised for each.

Large, voltage-independent, Aβ channels with clear open/closed step current transitions form in the presence of albumin-free oligomeric Aβ(1–42) assemblies, with channels found in 17 out of 49 (35%) patches, Figure 9. Similarly, a more dilute preparation of Aβ(1-42) oligomers (1 μM monomer equivalent) also causes ion channels to form in 9 out of 34 (26%) of patched pulled. A third oligomeric Aβ(1–42) preparation was then generated by incubation of Aβ (5 μM monomer equivalent) in the presence of HSA and these albumin trapped oligomers (characterized in Figure 2 and 3) were then applied to the membrane, Figure 9. We report that HSA-trapped oligomers were incapable of forming ion channels, with no channels formed in 18 patches of membrane. Aβ channels were also not present in 20 control patches of membrane exposed to Aβ-free buffer. Fisher's exact test confirmed channel formation by HSA-free Aβ(1-42) oligomers to be significant for both 1 μM ($p = 0.02$) and 5 μM ($p = 0.003$) Aβ preparations against HSA-trapped Aβ(1–42) oligomer.

DISCUSSION

HSA Inhibits Aβ Fibre Formation, Trapping Aβ in an Oligomeric Form, but Cannot Disassemble Pre-Formed Aβ Fibres

Aβ monomers, oligomers and fibres exist in a dynamic equilibrium, and fibres are the most thermodynamically stable structures [61]. The effect of binding partners on the equilibrium between these assemblies is of great interest [4], as the Aβ assembly state confers its cytotoxicity. Previous studies have shown that HSA inhibits fibre formation [9, 19-21]. There is disagreement as to whether HSA binds Aβ oligomers [20, 22, 62-64], or binds to Aβ trapping it in a monomeric state [15, 65]. The TEM images of albumin trapped Aβ oligomers shown here, indicates that albumin interacts with Aβ oligomers. These trapped oligomers are ~9 nm in diameter which approximates to ~270 kDa in size. We show that Aβ can be trapped in an oligomeric form which is incapable of forming ion-channels. The inability of albumin trapped Aβ oligomers to form ion-channels provides a mechanism by which HSA can have a protective role in Aβ's

cytotoxicity. This is supported by cell viability studies where the presence of albumin was able to reduce the cytotoxicity of Aβ(1-42) [19 24]. Thus, albumin may have a protective role in the brain as it can influence Aβ assembly outcomes at physiological μM concentrations.

Albumin has a moderate affinity for Aβ and it is reported to bind to Aβ monomer, or monomer-equivalent concentration of oligomer, with a dissociation constant of 5 μM [65] . Conversely, the affinity of Aβ monomer for growing fibre, described as the critical aggregation concentration (CAC), is reported to be approximately 100 nM for Aβ(1-40) [66, 67]. Despite Aβ having a tighter affinity for fibres, fibre growth of Aβ monomer (10 μM) was completely inhibited by HSA (20 μM) over a period of 38 days. One explanation for this behaviour may be that a true equilibrium has not been reached and Aβ is trapped in an off-pathway oligomeric form. Indeed we have recently shown that although Zn^{2+} has a weak affinity for Aβ, trace amounts of Zn^{2+} rapidly exchanging between multiple Aβ molecules can have a profound impact on assembly outcomes [68]. Alternatively, Milojevic *et al* [22 23] have reported that HSA binds Aβ oligomers with a tighter affinity (K_d = 1-100 nM). This implies the Aβ-HSA complex is thermodynamically more favourable than fibre elongation. If this is the case, then HSA should be able to shift the equilibrium towards favouring fibre disaggregation. However, we observed no significant decrease in ThT signal when Aβ fibres were incubated with HSA. We observed that even 200 μM HSA was unable to disassemble Aβ fibres over 22 days.

It is clear even after 22 or 38 days, a true equilibrium has not been reached either for pre-formed fibre disassembly by HSA, or Aβ fibres formed in the presence of HSA. Thus one of these reactions must be kinetically trapped. It has been shown that Aβ curvy-linear protofibrils and oligomers are able to dissociate into the monomeric form, taking 2 hrs for half of the oligomers to disassemble in the presence of a designed peptide fibre inhibitor [69]. However Aβ fibres are much more kinetically stable and their disassembly into monomers has an extremely slow rate constant, occurring only over many weeks [70]. It therefore seems probable that Aβ remains as a fibre as the rate of dissociation from Aβ fibres is very slow.

As well as albumin, there are a number of proteins that have been identified to inhibit fibre formation. These include the prion protein [6], extracellular chaperones such as clusterin [71, 72], designed peptides [69, 70], and other chaperone or non-chaperone proteins [5, 7]. These proteins inhibit Aβ fibre formation from monomer, but cellular prion protein (PrP^C) can disassemble preformed fibres over a few hours [6]. This suggests a very different mode of action for PrP^C

interacting with preformed fibres compared to albumin and other fibre growth inhibitors, which are mostly reported to influence the oligomeric and monomeric pool, but not preformed fibres.

Hydrophobic molecules that bind albumin, block albumin interaction with Aβ

Cholesterol and palmitic acid are endogenous hydrophobic molecules found in blood and ISF/CSF. These molecules bind to hydrophobic pockets within albumin [13, 39, 41] and have been linked with an increased risk of developing AD [43-48]. We have shown that when albumin is complexed with either of these ligands, the ability for albumin to inhibit Aβ fibrillisation is lost. Cholesterol and palmitic acid may compete with Aβ for binding to albumin, or their binding might induce a structural change in albumin which disrupts the Aβ binding site [23]. *In vivo* it is also possible that raised levels of cholesterol and fatty acids might impact albumins ability to bind Aβ. At μM CSF concentrations of albumin small variations in the capacity of HSA to bind Aβ found in the brain ISF/CSF is predicted to have a marked impact on Aβ fibre formation [9]. It is therefore conceivable that cholesterol/fatty acids binding to albumin could impact Aβ fibre formation in the brain interstitium, and also the ability of Aβ to form toxic oligomers that form ion channel pores. The observation that even sub-stoichiometric levels of cholesterol negate albumins protective properties supports a role for cholesterol. Interestingly, traumatic brain injury is also a risk factor for developing AD and is characterised by increased levels of saturated fatty acids in the brain, with palmitic acid levels increasing three-fold to 180 μM [73]. Fatty acids and cholesterol which bind to albumin may negate albumin's protective role and this hints at a possible mechanism through which fatty acids might heighten the risk of AD development, although other modes of action are also possible [55].

Albumin in blood serum and Aβ clearance from the CNS

In addition to the presence of albumin in the brain interstitium, HSA may also act as a protective sink for Aβ in blood serum [10, 11, 26] . As much as 25% of Aβ is cleared from the ISF/CSF across the blood-brain-barrier and furthermore, peripheral albumin levels regulate Aβ clearance [25]. As the most abundant protein in blood plasma (640 μM) albumin typically binds 90-95% of the Aβ found in blood plasma [14, 15]. High blood serum cholesterol at mid-life has been identified as an independent risk factor for developing AD [47, 48, 74]. The mechanisms by which blood cholesterol may increases AD risk are not yet resolved [55]; as cholesterol levels in the brain are unaffected by blood serum levels and cholesterol synthesis occurs within the brain

itself [75]. The observation that cholesterol will impede the binding of Aβ to albumin may therefore provide a mechanism in which blood serum cholesterol impacts AD. Similarly the high dietary intake of fats, particularly saturated fats, has been identified to increase the risk of developing AD [43, 44, 46]. While in AD mice models, a high fat diet leads to increases in cognitive impairment and Aβ deposition [76, 77]. Fatty acid binding to albumin is not exclusive to palmitic acid; the binding sites of several other fatty acids have also been identified, all of which share common hydrophobic binding pockets [41]. Indeed tetradecanoic acid has been shown to compete for Aβ binding to albumin [23]. It is likely that other fatty acids could therefore also supress the effect of HSA on Aβ fibrillisation. The various concentrations and μM affinities of a range of endogenous fatty-acids and cholesterol make their interplay with albumin a complex equilibrium in blood plasma and the CSF.

A number of hydrophobic therapeutic molecules also bind to HSA [78]. This raises the possibility that sustained use of, for example, the anti-coagulant warfarin might influence Aβ-HSA binding. The inhibitory effect of HSA on Aβ fibrillisation is lost by the addition of warfarin, where, like cholesterol and palmitic acid, warfarin disrupts the Aβ-HSA interaction. Thus wafarin might inhibit albumin's ability to act as a protective sink for Aβ, both in blood and possibly in the CSF. Warfarin is used as a long term preventative treatment against the formation of blood clots and against stroke. Studies have shown individuals with heart arrhythmia have an increased risk of developing AD [79-82], although we are not aware of any studies reported to show a link between AD and long-term warfarin use. A recent study shows a correlation between sustained the use of anticholinergic drugs and the onset of dementia [83]. Amongst these drugs are Doxepin and chlorphenamine that have been reported to bind to HSA [84]. It is possible that these drugs might also disrupt Aβ-albumin interaction.

CONCLUSIONS

In vitro albumin has a profound effect on Aβ fibre formation, even at μM concentrations found in the ISF/CSF. Our TEM images show Aβ is trapped by albumin in a relatively small range of oligomeric assemblies, 9 nm in diameter. These albumin associated Aβ oligomers are incapable of forming ion-channels, which provides a mechanism by which albumin may be protective against Aβ's cytotoxicity. Endogenous and exogenous hydrophobic molecules that

bind to albumin have an impact on albumin's role in Aβ fibrillisation. High cholesterol and fatty acids in the diet are known risk factors in the development of AD, raising the possibility that these risk factors are linked to their action on a neuroprotective albumin which acts as an Aβ sink in blood plasma. A potential therapeutic strategy recently explored is the clearance of Aβ from the CNS across the blood-brain-barrier using plasma exchange of albumin, which has shown efficacy in a phase-II clinical trial [36].

MATERIALS AND METHODS

Aβ production and solubilisation: Lyophilised Aβ(1-40) and Aβ(1-42) were purchased commercially from EZBiolab Inc. and Cambridge Research Biochemicals. Aβ peptides were synthesised using solid phase F-moc (N-(9-fluorenyl)methoxycarbonyl) chemistry, producing a single elution band in HPLC with correct mass verified by mass spectrometry. Aβ(1-40) and Aβ(1-42) were solubilised by dissolving 0.7 $mg.ml^{-1}$ Aβ in ultra-high quality (UHQ) water at pH 10 and rocked gently for 4 hrs at 4^{o}C. This procedure has been found to be an effective solubilisation protocol [85, 86]. It was necessary, particularly in the case of Aβ(1-42), to remove any remaining nucleating, oligomeric, aggregates by size exclusion chromatography (SEC) (Superdex 75 10/300 GL column, GE Healthcare) to generate a seed-free preparation. Based on a single elution peak in size exclusion chromatography, a clear lag-phase observed in fibre growth curves and a lack of detectable assemblies observed by TEM, SEC-eluted Aβ stock was deemed to be seed-free and monomeric. Aβ concentration was determined using the Tyrosine absorbance at 280 nm, ε_{280} =1280 M^{-1} cm^{-1}.

Human Serum Albumin (HSA): ≥99% Fatty acid and globulin-free HSA was purchased from Sigma-Aldrich Company Ltd. and solubilised in ultra-high quality (UHQ) water (10^{-18} $\Omega^{-1}cm^{-1}$ resistivity). The concentration was determined using the absorbance at 280 nm, ε_{280} = 34445 M^{-1} cm^{-1}. All other chemicals were purchased from Sigma-Aldrich Company Ltd.

Aβ Assembly Kinetics: Assembly kinetics were monitored by addition of 10 μM of the fluorescent dye, Thioflavin T (ThT). ThT fluoresces when bound to amyloid fibres to give a fluorescent signal proportional to the amount of amyloid fibre present, whilst ThT fluorescence for monomer and oligomeric assemblies is minimal [56]. ThT fluorescence was measured using BMG-Galaxy and BMG-Omega FLUOstar fluorescence 96-well plate readers. Flat-bottomed, polystyrene, non-tissue-culture treated plates were purchased from Falcon. Well plates were subjected to mild double orbital shaking for 30 s every 30 min followed by a fluorescence reading, 20 flashes per well per cycle with 4 mm orbital averaging. Fluorescence excitation and emission detection were at 440 and 490 nm, respectively. It has been shown that ThT does not markedly affect fibre formation kinetics or fibre morphology [56].

Conversion of the Aβ monomer into the fibre follows a characteristic sigmoidal fibre growth curve, which has a lag-phase (nucleation) and a growth-phase (elongation). The data obtained can be fit to the growth curve using the following equation:

$$Y = (y_i + m_i x) + \frac{y_f + m_f x}{1 + e^{-(\frac{x - xo}{\tau})}}$$

where *y* is the ThT fluorescence intensity, *x* is the time and x_o is the time at which the ThT fluorescence has reached half maximal intensity referred to as t_{50}. y_i and y_f are the initial and final fluorescence signals. The apparent fibre growth rate (k_{app} for elongation) is calculated from, $k_{app}=1/\tau$ and the lag-time (t_{lag}) is taken from $t_{lag}= X_o -2\tau$ [87]. The reciprocal of lag-time (t_{lag}) is largely influenced by the microscopic rate constants associated with a combination of primary and secondary nucleation as well as fragmentation, while the apparent fibre growth rate (k_{app}) is influenced by the elongation rate constant, due to the addition of each monomer onto a growing fibre [88].

Fibre growth curves were presented using KaleidaGraph. Kinetic parameters were extracted from, typically, 6 kinetic traces and the mean values and standard errors calculated. Analysis of variance (ANOVA) was used to compare the kinetic parameters extracted from curve fitting under different conditions. One-way ANOVA with Tukey-HSD post-hoc tests were used to reveal significant differences at P = 0.05.

Preparation of Aβ fibres and HSA-trapped oligomers: Amyloid fibre preparations of Aβ(1–40) and Aβ(1–42) were generated by incubation in a 96-well plate at 30°C. Aβ peptides were incubated at a concentration of 10 μM in 160 mM NaCl, and 30 mM HEPES buffer (pH 7.4). HSA (20 or 50 μM) was also added to adjacent wells of 10 μM Aβ incubated in identical pH 7.4 buffer. HSA was added to Aβ at three separate time-points of fibre growth assembly, those being at the beginning of fibre growth (0 hrs), at the end of the lag-phase and after maximal fibre formation (≥70 hrs).

Preparation of Aβ oligomer for patch-clamp: It was also necessary to generate an oligomeric Aβ(1–42) preparation in the absence of HSA which was previously reported to form toxic ion

channels [3]. Aβ(1–42) oligomer was obtained from the well plate towards the end of the lag-phase, as monitored by ThT fluorescent dye in separate wells and not used for ion channel measurements. Samples were immediately stored at -80 ^{o}C to prevent further assembly before use in patch-clamp experiments. HSA-free Aβ(1–42) oligomer was diluted into patch-clamp buffer before delivery to cell membrane at a final 5 μM preparation.

Transmission Electron Microscopy and Single Particle Analysis: Aβ-containing preparations, typically 5 μM to 0.05 μM Aβ monomer-equivalent concentration, were aliquoted (5 μl) onto glow-discharged carbon-coated 300 mesh grids using the droplet method and washed past with UHQ water. A negative stain phosphotungstic acid (2% (w/v), pH 7.4) was then applied before a final wash step and air-drying. Images were captured at 80,000 × using a JEOL model JEM-1230 electron microscope (JEOL, Ltd., Japan) operating at 80 keV, paired with a Morada 2k CCD camera system and its iTEM software package (Olympus Europa, UK). Representative single particle images of each oligomer were interactively selected using the e2boxer.py module of the EMAN2 software package [89] from multiple 16-bit micrograph CCD patches visualised from several grids and fields. All subsequent image processing was performed using the Imagic-5 environment. CCD patches from the Morada system were chosen that displayed minimal astigmatism and drift. The sampling frequency corresponded to 5.962 Å per pixel at the specimen level.

A data set of single particle images was obtained by picking all distinct particles by visual inspection, determined to be HSA-trapped Aβ(1-40) and Aβ(1-42) oligomers. This dataset was then subjected to single particle analysis, starting with the reference free alignment-by-classification procedure in order to identify 9 sub-populations of particles differing in size and shape. The diameter of the oligomers were assumed to be spherical to predict an approximate molecular mass using Calctool [90].

Single-Cell Fluorescence: Fibre growth and disassembly was followed using ThT Fluorescence. 10 μM Aβ(1-40) was incubated with 20 μM ThT in 160 mM NaCl and 30 mM HEPES, at pH 7.4. For recordings taken over a long time span, 0.005 % (w/v) sodium azide was added to prevent microbial growth. ThT measurements were conducted on a temperature-controlled Hitachi F-2500 fluorescence spectrophotometer at 30^{o}C. Excitation wavelength was set to 440 nm and an emission wavelength scan was collected between 460 nm and 650 nm in

order to measure peak-fluorescence. Samples were placed in a 1 cm quartz cuvette (Hellma) and three fluorescence readings were averaged at each time point. Readings were taken every day for up to 50 days with samples subjected to constant shaking at 30^{o}C. Between readings the samples remained covered and kept in the dark to reduce possible degradation of the fluorophore and microbial growth.

Cholesterol-Loaded and -Palmitic Acid-Loaded Albumin: Cholesterol was solubilised in dimethyl sulfoxide (DMSO) to generate a stock solution such that when diluted in aqueous buffer to the desired cholesterol concentration, the final DMSO concentration would be 2 % (v/100 ml). Each HSA monomer binds one cholesterol molecule [38]. An equimolar concentration of cholesterol and HSA (1:1) was used throughout. Cholesterol and HSA were pre-incubated together at room temperature to allow complex formation for a minimum of 30 min prior to use.

Palmitic acid was also solubilised in DMSO. HSA can bind up to 7 palmitic acid molecules [41], hence HSA was loaded with 7 molar equivalents of palmitic acid. Stocks of palmitic acid were mixed with HSA and diluted with water to bring the final DMSO concentration to 6 % (v/100 ml). Palmitic acid was incubated with HSA for 2.5 hrs at room temperature to allow for binding to occur before excess palmitic acid was removed through 5 concentration/dilution cycles. Samples were concentrated using 10 kDa MWCO centrifugal concentrators (Vivaspin, Sartorius) and the concentrated HSA-palmitic acid complex was returned to its original concentration by dilution into 6 % DMSO. Final concentrations of palmitic acid-loaded HSA used were then further diluted such that the well-plate incubated samples contained 2 % DMSO.

Warfarin-Loaded Albumin: Warfarin was solubilised in UHQ water. HSA is reported to bind up to 4 molecules of warfarin, thus 4 molar-equivalents of warfarin were incubated with HSA in 50 mM HEPES (pH 7.4). Aβ(1-40) at 10 μM was then incubated with 0, 20 and 30 μM HSA loaded with 4 molar-equivalents of warfarin. Additional controls of 10 μM Aβ(1-40) with 20 and 30 μM HSA, and of 10 μM Aβ(1-40) with 80 and 120 μM warfarin were also prepared.

Native-PAGE - PAGE was performed using Bio-Rad pre-cast gels and Bio-Rad Mini-Protean electrophoresis cells. Before separation, Aβ samples were concentrated (x4) using 5 kDa

MWCO centrifugal concentrators (Sartorius Vivaspin 500, Sartorius UK Ltd., Epsom, UK). Peptide preparations were then diluted into loading buffer at a ratio of 1:1 before electrophoresis on Bio-Rad 4–20% Mini-PROTEAN Tris-glycine gels (Bio-Rad Laboratories Ltd., Watford, UK). Gels were run at 40V for ~4 hrs before being stained with Coomassie Brilliant Blue R-250 (ThermoFisher Scientific Inc. USA).

Cell Culture: HEK293 immortal cells were cultured at 37°C within a 5% CO_2 incubator in Dulbecco's modified Eagle's medium (DMEM) supplemented with 10% foetal bovine serum, 200 units penicillin, and 0.2 $mg.ml^{-1}$ streptomycin. On reaching confluence, cells were dissociated from culture flasks using a Ca^{2+}- and Mg^{2+}-free phosphate-buffered saline (pH 7.2) solution. Cultured cells were split every 7 days and used between passages 80 and 85. With each round of splitting, a fraction of cells was plated into 35 mm diameter Petri dishes and maintained in supplemented DMEM until the day of any given patch clamp experiment. Plated cells were cultured for 2 to 5 days before use in patch clamp experiments. Reagents and media were purchased from Sigma-Aldrich Ltd., UK, and ThermoFisher Scientific (Invitrogen).

Patch Clamp Recording: Patch clamp recordings in voltage clamp mode were made from excised membranes of HEK293 cells. Patch pipettes were backfilled with patch clamp buffer containing Aβ preparations at 1 and 5 μM monomer equivalent concentration of Aβ (pH 7.4). Backfilled Aβ diffused toward the extracellular face of the membrane within the patch pipette. The membrane was then excised and clamped at a series of voltage potentials between +60 and -60 mV and transmembrane currents were measured. Patches of membrane were excised, in an inside-out configuration, submersed in a 35 mm dish containing buffer of identical ionic composition. A stepwise voltage ramp protocol was applied using an Axopatch 200B amplifier (Axon Instruments, Union City, CA) via personal computer using PCLAMP-10 software (Axon Instruments). Data were further processed and analysed using the Clampfit software package and a low pass boxcar filter was typically applied. Patches were pulled from thick walled filament borosilicate glass (Harvard Apparatus, Edenbridge, Kent, UK) with a needle diameter of ~1 to 3 μm and a resistance of 4 to 6 MΩ (megaohms) when filled with recording solution. Junction potentials generated at boundaries of ionic asymmetry were accounted for using an applied pipette offset potential. Recordings were sampled at a rate of 2 kHz with 500 μs intervals with a low pass four-pole Bessel filter frequency of 1 kHz. In the excised patch, the holding potential was set to 0 mV. Recordings were made in symmetrical solution adjusted to

pH 7.4 containing 121.4 mM NaCl, 10 mM CsCl, 9 mM Na-HEPES, 1.85 mM $CaCl_2$, 1.87 mM $MgCl_2$, 2.16 mM KCl. Transmembrane patch currents were recorded for 30 min; when current spikes, indicative of membrane destabilization, were observed in this period, the recordings were extended to 45 min.

Acknowledgments: Funding from the BBSRC, grant no. BB/M023877/1 and Queen Mary- life sciences initiative.

Conflict of interest: The authors declare that they have no conflicts of interest with the contents of this article.

Author Contribution: DCB contributed equally to experimental work (Figures: 1; 2; 3; 6; 8; 9). HFS contributed equally to experimental work (Figures: 4; 5; 6; 7). TPLH contributed equally to experimental work (Figures: 4; 5; 8). MDB supervised ion-channel studies. JN preformed TEM single particle analysis. JHV conceived of the study and supervised the studies. All authors reviewed the results and approved the final version of the manuscript.

Figure Legends:

Figure 1: HSA inhibits Aβ fibre growth and impedes elongation of Aβ oligomers**.** Fibre growth kinetics were monitored for Aβ(1-40) in the presence and absence of HSA. ThT fluorescence was recorded over 70 hrs under 3 conditions, Aβ(1-40) (blue), Aβ(1-40) with HSA at 0 hrs (red) and Aβ(1-40) with HSA at the beginning of fibre growth phase (green). The green arrow indicates addition of HSA after 28 hrs of Aβ incubation. Final peptide concentrations were 10 μM Aβ and 50 μM HSA. Preparations were incubated with 10 μM ThT, 30 mM HEPES buffer, 160 mM NaCl and 0.005 (g/100 ml) sodium azide, at pH 7.4. n = 6 traces for each condition

Figure 2: Albumin traps Aβ as spherical oligomers, but does not disassemble pre-formed fibres. Negative-stain TEM micrographs were obtained for preparations of Aβ(1-40) and Aβ(1-42) incubated in the presence and absence of albumin. An absence of oligomeric assemblies was confirmed in three control preparations of **(a)** Aβ(1-40) monomer, **(b)** Aβ(1-42) monomer, and **(c)** HSA alone. Spherical HSA-trapped oligomers ~ 10nm in diameter were observed after 100 hours of incubation in preparations where HSA was added to: **(d)** monomeric Aβ(1-40), **(e)** oligomeric Aβ(1-40), at the end of the lag phase, and **(f)** monomeric Aβ(1-42)**.** However, fibre morphology appears to be unchanged when HSA is added to pre-formed fibre preparations, with no apparent difference between Aβ(1-40) and Aβ(1-42) control samples **(g)**,**(i)** and Aβ(1-40) fibres in the presence of HSA **(h)**. Preparations were at 10 μM Aβ and 50 μM HSA and incubated with Aβ for 100 hours in 30 mM HEPES at pH 7.4, 160 mM NaCl.

Figure 3: TEM views of Aβ(1-40) and Aβ(1-42) albumin-trapped oligomers. Three representative class averages taken from 368 and 210 manually picked oligomers for Aβ(1-40) and Aβ(1-42). Each class average represents between 27 and 67 particles. Analysis was performed on micrographs of negatively stained Aβ (10 μM) incubated with HSA (50 μM) for 70 hours. Diameters ranged between ~8 and ~10 nm.

Figure 4: HSA inhibits Aβ fibre formation over 38 Days. Inhibition of Aβ(1-40) fibre growth was monitored by recording ThT fluorescence over 38 days. In the absence of HSA, maximal Aβ(1-40) fibre formation is observed within 48 hrs. However, when HSA is added to monomeric Aβ(1-40), fibre growth is inhibited. Fluorescence emission spectra taken over a 38 day period: (a) Aβ alone and (b) Aβ in the presence of HSA. ThT fluorescence (at 485 nm) has been plotted against time (c). Final peptide concentrations were 10 μM Aβ and 20 μM HSA. Preparations were incubated with 30 mM HEPES, 160 mM NaCl and 0.005 (g/100 ml) sodium azide, at pH 7.4, at 30 ^{o}C Two repeat experiments shown for growth conditions.

Figure 5: HSA does not disaggregate pre-formed Aβ fibres over 22 Days. A high stability of Aβ(1-40) fibres is confirmed in the presence of HSA. Aβ(1-40) fibre formation was observed by ThT fluorescence, and identical fibre preparations were generated. ThT fluorescence was then recorded over a period of 22 days to monitor the presence of pre-formed Aβ(1-40) fibres (10 μM monomer equivalent) in the presence of 0, 3, 20 and 200 μM HSA. The ThT signal remains stable in the presence of HSA and suggests fibre content is constant throughout. All samples were incubated with 30 mM HEPES, 160 mM NaCl and 0.005 (g/100 ml) sodium azide, at pH 7.4.

Figure 6: Cholesterol negates HSA-mediated inhibition of Aβ(1-40) fibre formation. Aβ(1-40) (10 μM) fibre formation monitored by ThT fluorescence over time. (a) Aβ(1-40) in HEPES buffer with and without 2 % (v/v) DMSO, (b) Aβ(1-40) in presence of albumin (20 μM), (c) Aβ(1-40) in the presence of (1:1) cholesterol-loaded albumin (20 μM). (d) Negative-stain TEM image of Aβ(1-40) fibres formed in the presence of cholesterol-loaded albumin, scale bar = 100 nm. All samples were incubated with 20 μM ThT, 30 mM HEPES at pH 7.4, 160 mM NaCl and 0.005 (g/100 ml) sodium azide. n = 6 traces for each condition.

Figure 7: Aβ(1-40) fibre growth returns in the presence of palmitic acid loaded-HSA. Aβ(1-40) (10 μM) fibre formation monitored by ThT fluorescence over time. (a) Aβ(1-40) in HEPES buffer with and without 2 % (v/v) DMSO, (b) Aβ(1-40) in presence of 10 μM fatty acid free albumin, (c) Aβ(1-40) in the presence of palmitic acid loaded albumin (10 μM). All samples

were incubated with 30 mM HEPES, 20 μM ThT, 160 mM NaCl and 0.005 (g/100 ml) sodium azide, at pH 7.4. n = 6 traces for each condition.

Figure 8: Aβ(1-40) fibre growth is observed in the presence of Warfarin-loaded HSA**.** ThT fluorescence was monitored over time to observe fibre formation. (a) Aβ(1-40) alone, (b) Aβ(1-40) incubated with HSA (30 μM) and (c) Aβ(1-40) incubated with HSA (30 μM) loaded with warfarin (120 μM). (d) Negative-stain TEM image of Aβ(1-40) fibres formed in the presence of warfarin-loaded albumin, scale bar = 50 nm. All Aβ(1-40) samples were at a concentration of 10 μM and incubated with 30 mM HEPES, 20 μM ThT, 160 mM NaCl and 0.005 % (w/v) sodium azide, at pH 7.4. n = 5 traces for each condition.

Figure 9: HSA prevents ion channel formation by Aβ(1-42) in the cellular membrane. Preparations of Aβ(1-42) oligomer were generated in the presence and absence of HSA and presented to excised extracellular membrane surface. Transmembrane current was then recorded over a range of potentials, and a representative recorded current trace is shown with corresponding TEM images for preparations containing **(a)** Aβ(1-42) oligomer; **(b)** HSA-trapped Aβ(1-42) oligomer. **(c)** The bar-chart shows the proportion of membrane patches that formed ion channels in the presence of Aβ(1-42) oligomer and HSA-trapped Aβ(1-42) oligomer. Channel formation was significant for both 1 μM (n = 34) and 5 μM (n = 49) concentrations of Aβ(1–42) oligomer, against corresponding HSA-trapped Aβ(1–42) oligomer preparations which were unable to form ion channels within 30 min (n = 18). 5 molar equivalences of HSA was used to generate HSA-trapped oligomers. **(d)** Shows voltage ramp protocol which was applied to clamp the cell membrane at six membrane potentials between -60 and +60 mV.

REFERENCES

1. Prince M., Wimo A., Guerchet M., Gemma-Claire A., Wu Y.-T. & Prina M. (2015). World Alzheimer Report 2015: The Global Impact of Dementia - An analysis of prevalence, incidence, cost and trends. Alzheimer's Disease International. 84.
2. Hardy J. & Selkoe D. J. (2002). Medicine - The amyloid hypothesis of Alzheimer's disease: Progress and problems on the road to therapeutics. Science. 297, 353-6.
3. Bode D. C., Baker M. D. & Viles J. H. (2017). Ion Channel Formation by Amyloid-β42 Oligomers but Not Amyloid-β40 in Cellular Membranes. J Biol Chem. 292, 1404-13.
4. Han S. H., Park J. C. & Mook-Jung I. (2016). Amyloid β-interacting partners in Alzheimer's disease: From accomplices to possible therapeutic targets. Prog Neurobiol. 137, 17-38.
5. Luo J., Wärmländer S. K., Gräslund A. & Abrahams J. P. (2014). Non-chaperone proteins can inhibit aggregation and cytotoxicity of Alzheimer amyloid β peptide. J Biol Chem. 289, 27766-75.
6. Younan N. D., Sarell C. J., Davies P., Brown D. R. & Viles J. H. (2013). The cellular prion protein traps Alzheimer's Abeta in an oligomeric form and disassembles amyloid fibers. FASEB J. 27, 1847-58.
7. Härd T. & Lendel C. (2012). Inhibition of amyloid formation. J Mol Biol. 421, 441-65.
8. Viles J. H. (2012). Metal ions and amyloid fiber formation in neurodegenerative diseases. Copper, zinc and iron in Alzheimer's, Parkinson's and prion diseases. Coordination Chemistry Reviews. 256, 2271-84.
9. Stanyon H. F. & Viles J. H. (2012). Human Serum Albumin Can Regulate Amyloid-β Peptide Fiber Growth in the Brain Interstitium: IMPLICATIONS FOR ALZHEIMER DISEASE. J Biol Chem. 287, 28163-8.
10. Yamamoto K., Shimada H., Koh H., Ataka S. & Miki T. (2014). Serum levels of albumin-amyloid beta complexes are decreased in Alzheimer's disease. Geriatr Gerontol Int. 14, 716-23.
11. Kim T.-S., Pae C.-U., Yoon S.-J., Jang W.-Y., Lee N. J., Kim J.-J., et al. (2006). Decreased plasma antioxidants in patients with Alzheimer's disease. International Journal of Geriatric Psychiatry. 21, 344–8.
12. Llewellyn D. J., Langa K. M., Friedland R. P. & Lang I. A. (2010). Serum albumin concentration and cognitive impairment. Curr Alzheimer Res. 7, 91-6.
13. Carter D. & Ho J. (1994). Structure of serum albumin. Advances in protein chemistry. 45, 153-203.
14. Biere A. L., Ostaszewski B., Stimson E. R., Hyman B. T., Maggio J. E. & Selkoe D. J. (1996). Amyloid β-Peptide Is Transported on Lipoproteins and Albumin in Human Plasma. J Biol Chem. 271, 32916-22.
15. Kuo Y.-M., Kokjohn T. A., Kalback W. M., Luehrs D., Galasko D. R., Chevallier N., et al. (2000). Amyloid-beta Peptides Interact with Plasma Proteins and Erythrocytes: Implications for Their Quantitation in Plasma. Biochem Biophys Res Commun. 268, 750-6.
16. Seubert P., Vigo-Pelfrey C., Esch F., Lee M., Dovey H., Davis D., et al. (1992). Isolation and quantification of soluble Alzheimer's β-peptide from biological fluids. Nature. 359, 325-7.
17. Lame M. E., Chambers E. E. & Blatnik M. (2011). Quantitation of amyloid beta peptides Aβ1–38, Aβ1–40, and Aβ1–42 in human cerebrospinal fluid by ultra-performance liquid chromatography–tandem mass spectrometry. Anal Biochem. 419, 133-9.
18. Stevens R., Elmendorf D., Gourlay M., Stroebel E. & Gaafar H. (1979). Application of fluoroimmunoassay to cerebrospinal fluid immunoglobulin G and albumin. Journal of Clinical Microbiology. 10, 346-50.
19. Wang C., Cheng F., Xu L. & Jia L. (2016). HSA targets multiple Abeta 42 species and inhibits the seeding-mediated aggregation and cytotoxicity of Abeta 42 aggregates. RSC ADVANCES. 6, 71165-75.
20. Reyes Barcelo A., Gonzalez-Velasquez F. & Moss M. (2009). Soluble aggregates of the amyloid-beta peptide are trapped by serum albumin to enhance amyloid-beta activation of endothelial cells. Journal of Biological Engineering. 3, 5-12.
21. Bohrmann B., Tjernberg L., Kuner P., Poli S., Levet-Trafit B., Näslund J., et al. (1999). Endogenous proteins controlling amyloid beta-peptide polymerization. Possible implications for beta-amyloid formation in the central nervous system and in peripheral tissues. J Biol Chem. 274, 15990-5.
22. Milojevic J. & Melacini G. (2011). Stoichiometry and affinity of the human serum albumin-Alzheimer's Abeta peptide interactions. Biophys J. 100, 183-92.
23. Algamal M., Milojevic J., Jafari N., Zhang W. & Melacini G. (2013). Mapping the Interactions between the Alzheimer’s A< i> β</i>-Peptide and Human Serum Albumin beyond Domain Resolution. Biophys J. 105, 1700-9.
24. Domínguez-Prieto M., Velasco A., Vega L., Tabernero A. & Medina J. M. (2017). Aberrant Co-localization of Synaptic Proteins Promoted by Alzheimer's Disease Amyloid-β Peptides: Protective Effect of Human Serum Albumin. J Alzheimers Dis. 55, 171-82.

25. Marques M. A., Kulstad J. J., Savard C. E., Green P. S., Lee S. P., Craft S., et al. (2009). Peripheral amyloid-beta levels regulate amyloid-beta clearance from the central nervous system. J Alzheimers Dis. 16, 325-9.
26. Tanzi R. E., Moir R. D. & Wagner S. L. (2004). Clearance of Alzheimer's Abeta peptide: the many roads to perdition. Neuron. 43, 605-8.
27. DeMattos R. B., Bales K. R., Cummins D. J., Paul S. M. & Holtzman D. M. (2002). Brain to plasma amyloid-beta efflux: a measure of brain amyloid burden in a mouse model of Alzheimer's disease. Science. 295, 2264-7.
28. Zlokovic B. V. (2004). Clearing amyloid through the blood–brain barrier. Journal of Neurochemistry. 89, 807–11.
29. Roberts K. F., Elbert D. L., Kasten T. P., Patterson B. W., Sigurdson W. C., Connors R. E., et al. (2014). Amyloid-β efflux from the central nervous system into the plasma. Ann Neurol. 76, 837-44.
30. Wang Y. R., Wang Q. H., Zhang T., Liu Y. H., Yao X. Q., Zeng F., et al. (2017). Associations Between Hepatic Functions and Plasma Amyloid-Beta Levels-Implications for the Capacity of Liver in Peripheral Amyloid-Beta Clearance. Mol Neurobiol. 54, 2338-44.
31. Ezra A., Rabinovich-Nikitin I., Rabinovich-Toidman P. & Solomon B. (2016). Multifunctional Effect of Human Serum Albumin Reduces Alzheimer's Disease Related Pathologies in the 3xTg Mouse Model. J Alzheimers Dis. 50, 175-88.
32. Boada M., Ortiz P., Anaya F., Hernandez I., Muñoz J., Núñez L., et al. (2009). Amyloid-Targeted Therapeutics in Alzheimer's Disease: Use of Human Albumin in Plasma Exchange As a Novel Approach for A beta Mobilization. Drug News Perspect. 22, 325-39.
33. Henderson S. J., Andersson C., Narwal R., Janson J., Goldschmidt T. J., Appelkvist P., et al. (2014). Sustained peripheral depletion of amyloid-β with a novel form of neprilysin does not affect central levels of amyloid-β. Brain. 137, 553-64.
34. Boada M., Ramos-Fernández E., Guivernau B., Muñoz F. J., Costa M., Ortiz A. M., et al. (2016). Treatment of Alzheimer disease using combination therapy with plasma exchange and haemapheresis with albumin and intravenous immunoglobulin: Rationale and treatment approach of the AMBAR (Alzheimer Management By Albumin Replacement) study. Neurologia. 31, 473-81.
35. Costa M., Ortiz A. M. & Jorquera J. I. (2012). Therapeutic albumin binding to remove amyloid-β. J Alzheimers Dis. 29, 159-70.
36. Boada M., Anaya F., Ortiz P., Olazarán J., Shua-Haim J. R., Obisesan T. O., et al. (2017). Efficacy and Safety of Plasma Exchange with 5% Albumin to Modify Cerebrospinal Fluid and Plasma Amyloid-β Concentrations and Cognition Outcomes in Alzheimer's Disease Patients: A Multicenter, Randomized, Controlled Clinical Trial. J Alzheimers Dis. 56, 129-43.
37. Drew L. (2017). Neuroscience: The power of plasma. Nature. 549, S26-S7.
38. Peng L., Minbo H., Fang C., Xi L. & Chaocan Z. (2008). The interaction between cholesterol and human serum albumin. Protein Pept Lett. 15, 360-4.
39. Teir M. A., Ghithan J., Darwish S. & Abu-Hadid M. M. (2012). Multi-Spectroscopic Investigation of the Interactions between Cholesterol and Human Serum Albumin. Journal of Applied Biological Sc. 6, 45-55.
40. Ashbrook J. D., Spector A. A., Santos E. C. & Fletcher J. (1975). Long chain fatty acid binding to human plasma albumin. J Biol Chem. 250, 2333-8.
41. Bhattacharya A. A., Grüne T. & Curry S. (2000). Crystallographic analysis reveals common modes of binding of medium and long-chain fatty acids to human serum albumin. J Mol Biol. 303, 721-32.
42. Petitpas I., Bhattacharya A. A., Twine S., East M. & Curry S. (2001). Crystal structure analysis of warfarin binding to human serum albumin: anatomy of drug site I. J Biol Chem. 276, 22804-9.
43. Laitinen M., Ngandu T., Rovio S., Helkala E.-L., Uusitalo U., Viitanen M., et al. (2006). Fat intake at midlife and risk of dementia and Alzheimer's disease: a population-based study. Dementia and geriatric cognitive disorders. 22, 99-107.
44. Morris M., Evans D. A., Bienias J. L. & et al. (2003). Dietary fats and the risk of incident alzheimer disease. Archives of Neurology. 60, 194-200.
45. Solomon A., Kåreholt I., Ngandu T., Winblad B., Nissinen A., Tuomilehto J., et al. (2007). Serum cholesterol changes after midlife and late-life cognition Twenty-one-year follow-up study. Neurology. 68, 751-6.
46. Kalmijn S., Launer L. J., Ott A., Witteman J., Hofman A. & Breteler M. (1997). Dietary fat intake and the risk of incident dementia in the Rotterdam Study. Annals of neurology. 42, 776-82.

47. Whitmer R. A., Sidney S., Selby J., Johnston S. C. & Yaffe K. (2005). Midlife cardiovascular risk factors and risk of dementia in late life. Neurology. 64, 277-81.
48. Notkola I., Sulkava R., Pekkanen J., Erkinjuntti T., Ehnholm C., Kivinen P., et al. (1998). Serum total cholesterol, apolipoprotein E epsilon 4 allele, and Alzheimer's disease. Neuroepidemiology. 17, 14-20.
49. Jones L., Holmans P. A., Hamshere M. L., Harold D., Moskvina V., Ivanov D., et al. (2010). Genetic Evidence Implicates the Immune System and Cholesterol Metabolism in the Aetiology of Alzheimer's Disease. PLoS ONE. 5, e13950.
50. Wollmer M. A. (2010). Cholesterol-related genes in Alzheimer's disease. Biochim Biophys Acta, Mol Cell Biol Lipids. 1801, 762-73.
51. Lütjohann D., Breuer O., Ahlborg G., Nennesmo I., Siden A., Diczfalusy U., et al. (1996). Cholesterol homeostasis in human brain: evidence for an age-dependent flux of 24S-hydroxycholesterol from the brain into the circulation. Proc Natl Acad Sci U S A. 93, 9799-804.
52. Sparks D. L., Scheff S. W., Hunsaker III J. C., Liu H., Landers T. & Gross D. R. (1994). Induction of Alzheimer-like β-amyloid immunoreactivity in the brains of rabbits with dietary cholesterol. Experimental neurology. 126, 88-94.
53. Refolo L. M., Pappolla M. A., Malester B., LaFrancois J., Bryant-Thomas T., Wang R., et al. (2000). Hypercholesterolemia accelerates the Alzheimer's amyloid pathology in a transgenic mouse model. Neurobiology of disease. 7, 321-31.
54. Hooijmans C. R., Van der Zee C. E. E. M., Dederen P. J., Brouwer K. M., Reijmer Y. D., van Groen T., et al. (2009). DHA and cholesterol containing diets influence Alzheimer-like pathology, cognition and cerebral vasculature in APPswe/PS1dE9 mice. Neurobiology of Disease. 33, 482-98.
55. Wood W. G., Li L., Müller W. E. & Eckert G. P. (2014). Cholesterol as a causative factor in Alzheimer's disease: a debatable hypothesis. J Neurochem. 129, 559-72.
56. Younan N. D. & Viles J. H. (2015). A Comparison of Three Fluorophores for the Detection of Amyloid Fibers and Prefibrillar Oligomeric Assemblies. ThT (Thioflavin T); ANS (1-Anilinonaphthalene-8-sulfonic Acid); and bisANS (4,4 '-Dianilino-1,1 '-binaphthyl-5,5 '-disulfonic Acid). Biochemistry. 54, 4297-306.
57. Sen P., Fatima S., Ahmad B. & Khan R. H. (2009). Interactions of thioflavin T with serum albumins: spectroscopic analyses. Spectrochim Acta A Mol Biomol Spectrosc. 74, 94-9.
58. Barritt J. D., Younan N. D. & Viles J. H. (2017). N-Terminally Truncated Amyloid-β(11-40/42) Co-Fibrillises with its Full-Length Counterpart, Implications for Alzheimer's Disease. Angewandte Chemie
59. Kivipelto M., Helkala E.-L., Laakso M. P., Hänninen T., Hallikainen M., Alhainen K., et al. (2002). Apolipoprotein E ε4 allele, elevated midlife total cholesterol level, and high midlife systolic blood pressure are independent risk factors for late-life Alzheimer disease. Annals of Internal Medicine. 137, 149-55.
60. Deliconstantinos G., Tsopanakis C., Karayiannakos P. & Skalkeas G. (1986). Evidence for the existence of non-esterified cholesterol carried by albumin in rat serum. Atherosclerosis. 61, 67-75.
61. Sánchez L., Madurga S., Pukala T., Vilaseca M., López-Iglesias C., Robinson C. V., et al. (2011). Aβ40 and Aβ42 amyloid fibrils exhibit distinct molecular recycling properties. J Am Chem Soc. 133, 6505-8.
62. Milojevic J., Costa M., Ortiz A. M., Jorquera J. I. & Melacini G. (2014). In Vitro Amyloid-β Binding and Inhibition of Amyloid-β Self-Association by Therapeutic Albumin. Journal of Alzheimer's Disease. 38, 753-65.
63. Milojevic J., Esposito V., Das R. & Melacini G. (2007). Understanding the Molecular Basis for the Inhibition of the Alzheimer's Aβ-Peptide Oligomerization by Human Serum Albumin Using Saturation Transfer Difference and Off-Resonance Relaxation NMR Spectroscopy. J Am Chem Soc. 129, 4282-90.
64. Milojevic J., Raditsis A. & Melacini G. (2009). Human Serum Albumin Inhibits A[beta] Fibrillization through a "Monomer-Competitor" Mechanism. Biophys J. 97, 2585-94.
65. Rózga M., Kloniecki M., Jablonowska A., Dadlez M. & Bal W. (2007). The binding constant for amyloid A[beta]40 peptide interaction with human serum albumin. Biochem Biophys Res Commun. 364, 714-8.
66. Iljina M., Garcia G. A., Dear A. J., Flint J., Narayan P., Michaels T. C., et al. (2016). Quantitative analysis of co-oligomer formation by amyloid-beta peptide isoforms. Sci Rep. 6, 28658.
67. O'Nuallain B., Shivaprasad S., Kheterpal I. & Wetzel R. (2005). Thermodynamics of A beta(1-40) amyloid fibril elongation. Biochemistry. 44, 12709-18.
68. Matheou C. J., Younan N. D. & Viles J. H. (2016). The Rapid Exchange of Zinc(2+) Enables Trace Levels to Profoundly Influence Amyloid-β Misfolding and Dominates Assembly Outcomes in Cu(2+)/Zn(2+) Mixtures. J Mol Biol. 428, 2832-46.

69. Grüning C. S., Klinker S., Wolff M., Schneider M., Toksöz K., Klein A. N., et al. (2013). The off-rate of monomers dissociating from amyloid-β protofibrils. J Biol Chem. 288, 37104-11.
70. Luheshi L. M., Hoyer W., de Barros T. P., van Dijk Härd I., Brorsson A. C., Macao B., et al. (2010). Sequestration of the Abeta peptide prevents toxicity and promotes degradation in vivo. PLoS Biol. 8, e1000334.
71. Narayan P., Meehan S., Carver J. A., Wilson M. R., Dobson C. M. & Klenerman D. (2012). Amyloid-beta oligomers are sequestered by both intracellular and extracellular chaperones. Biochemistry. 51, 9270-6.
72. Narayan P., Orte A., Clarke R. W., Bolognesi B., Hook S., Ganzinger K. A., et al. (2012). The extracellular chaperone clusterin sequesters oligomeric forms of the amyloid-beta(1-40) peptide. Nat Struct Mol Biol. 19, 79-83.
73. Lipton P. Ischemic Cell Death in Brain Neurons1999.
74. Kivipelto M., Helkala E.-L., Laakso M. P., Hänninen T., Hallikainen M., Alhainen K., et al. (2001). Midlife vascular risk factors and Alzheimer's disease in later life: longitudinal, population based study. Bmj. 322, 1447-51.
75. Chobanian A. V. & Hollander W. (1962). Body cholesterol metabolism in man. I. The equilibration of serum and tissue cholesterol. Journal of Clinical Investigation. 41, 1732.
76. Maesako M., Uemura K., Kubota M., Kuzuya A., Sasaki K., Asada M., et al. (2012). Environmental enrichment ameliorated high-fat diet-induced Aβ deposition and memory deficit in APP transgenic mice. Neurobiology of Aging. 33, 1011.e11-.e23.
77. Maesako M., Uemura K., Kubota M., Kuzuya A., Sasaki K., Hayashida N., et al. (2012). Exercise is more effective than diet control in preventing high fat diet-induced β-amyloid deposition and memory deficit in amyloid precursor protein transgenic mice. J Biol Chem. 287, 23024-33.
78. Ghuman J., Zunszain P. A., Petitpas I., Bhattacharya A. A., Otagiri M. & Curry S. (2005). Structural Basis of the Drug-binding Specificity of Human Serum Albumin. J Mol Biol. 353, 38-52.
79. Ott A., Breteler M. M., de Bruyne M. C., van Harskamp F., Grobbee D. E. & Hofman A. (1997). Atrial fibrillation and dementia in a population-based study. The Rotterdam Study. Stroke. 28, 316-21.
80. Barber M., Tait R. C., Scott J., Rumley A., Lowe G. D. & Stott D. J. (2004). Dementia in subjects with atrial fibrillation: hemostatic function and the role of anticoagulation. J Thromb Haemost. 2, 1873-8.
81. Ettorre E., Cicerchia M., De Benedetto G., Fossati C., Guglielmi S., Manzon L., et al. (2009). A possible role of atrial fibrillation as a risk factor for dementia. Arch Gerontol Geriatr. 49 Suppl 1, 71-6.
82. Jacobs V., Cutler M. J., Day J. D. & Bunch J. T. (2015). Atrial fibrillation and dementia. Trends in Cardiovascular Medicine. 25, 44-51.
83. Gray S. L., Anderson M. L., Dublin S., Hanlon J. T., Hubbard R., Walker R., et al. (2015). Cumulative use of strong anticholinergics and incident dementia: a prospective cohort study. JAMA Intern Med. 175, 401-7.
84. Valko K., Nunhuck S., Bevan C., Abraham M. H. & Reynolds D. P. (2003). Fast gradient HPLC method to determine compounds binding to human serum albumin. Relationships with octanol/water and immobilized artificial membrane lipophilicity. J Pharm Sci. 92, 2236-48.
85. Fezoui Y., Hartley D. M., Harper J. D., Khurana R., Walsh D. M., Condron M. M., et al. (2000). An improved method of preparing the amyloid beta-protein for fibrillogenesis and neurotoxicity experiments. Amyloid. 7, 166-78.
86. Teplow D. B. (2006). Preparation of amyloid beta-protein for structural and functional studies. Method Enzymol. 413, 20-33.
87. Uversky V. N., Li J. & Fink A. L. (2001). Metal-triggered structural transformations, aggregation, and fibrillation of human alpha-synuclein. A possible molecular NK between Parkinson's disease and heavy metal exposure. J Biol Chem. 276, 44284-96.
88. Meisl G., Kirkegaard J. B., Arosio P., Michaels T. C., Vendruscolo M., Dobson C. M., et al. (2016). Molecular mechanisms of protein aggregation from global fitting of kinetic models. Nat Protoc. 11, 252-72.
89. Tang G., Peng L., Baldwin P. R., Mann D. S., Jiang W., Rees I., et al. (2007). EMAN2: an extensible image processing suite for electron microscopy. J Struct Biol. 157, 38-46.
90. Shipway A. & Shipway S. Calctool: Protein Size. 2008.

Highlights:

Albumin binds to Aβ inhibiting fibre formation at physiological (μM) concentrations.

TEM indicates albumin kinetically traps Aβ as oligomers, 9 nm in diameter.

Albumin-trapped Aβ oligomeric assemblies are incapable of forming ion-channels.

Cholesterol, warfarin & fatty acids (FAs) suppress albumin's amyloid inhibiting properties.

Aβ clearance from the brain by albumin may be impacted by cholesterol and FAs levels.

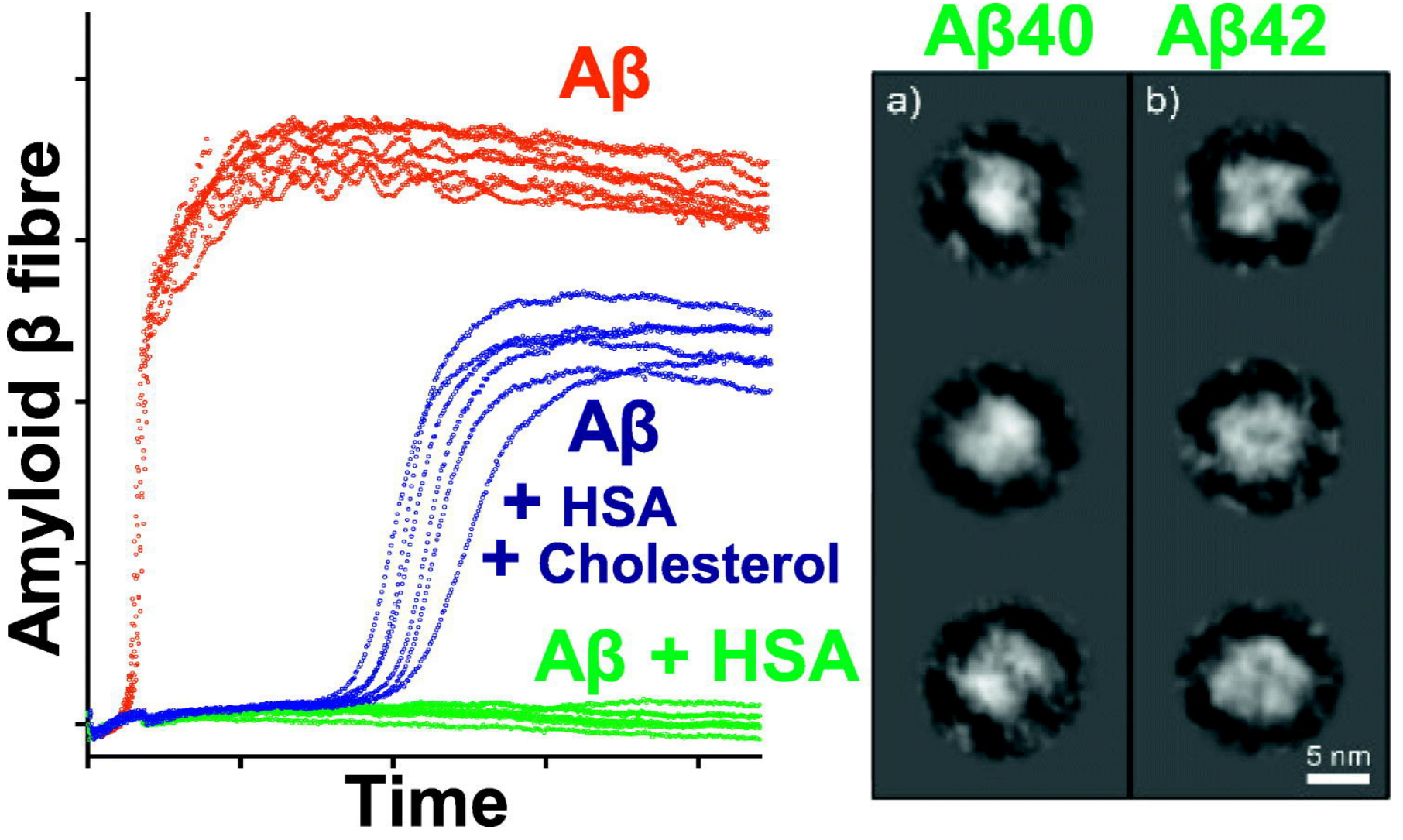

Graphics Abstract

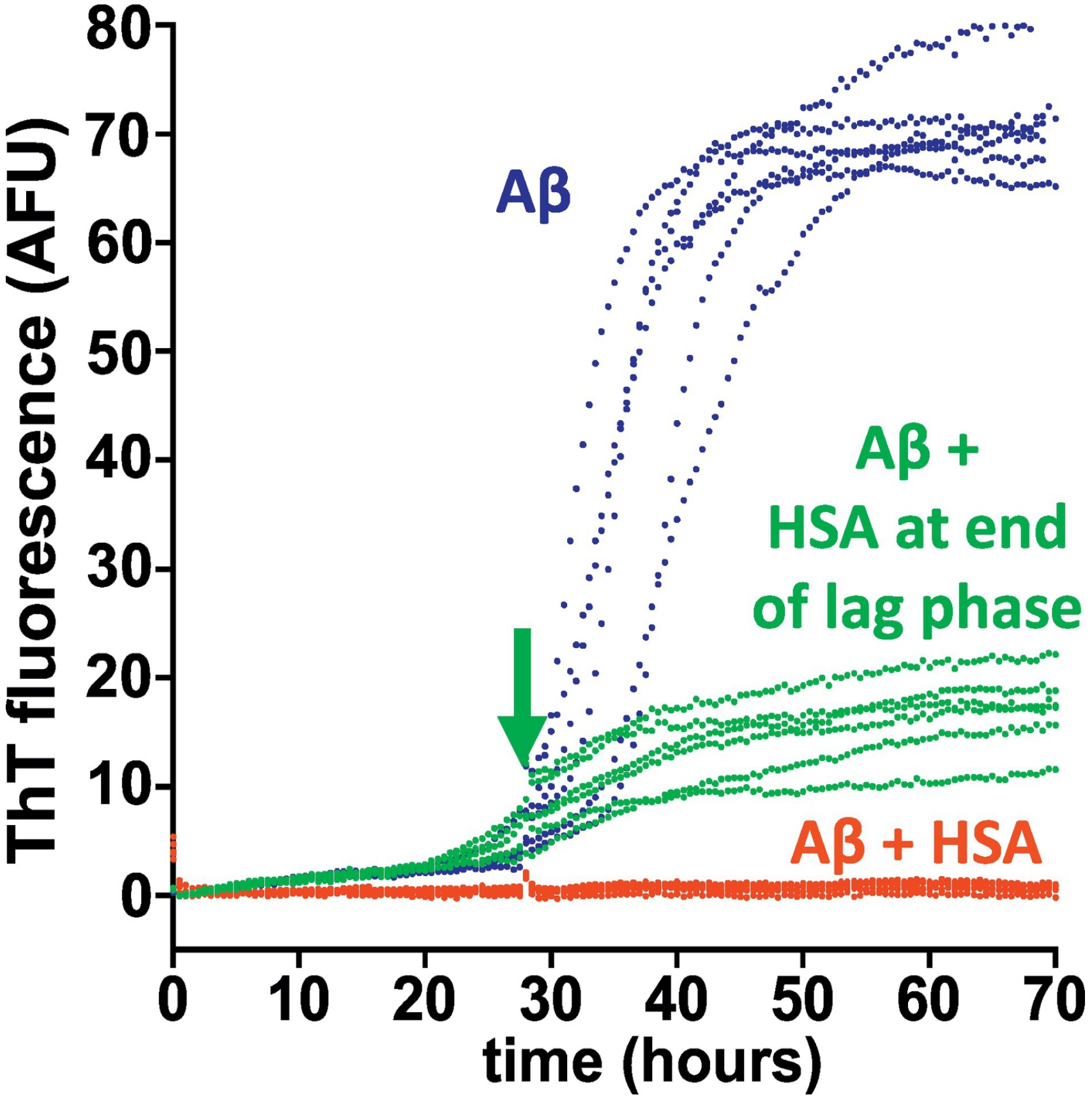
ThT fluorescence (AFU)
80
70
60
50
40
30
20
10
0
0
10
20
30
40
50
60
70
time (hours)
Aβ
Aβ +
HSA at end
of lag phase
Aβ + HSA

Figure 1

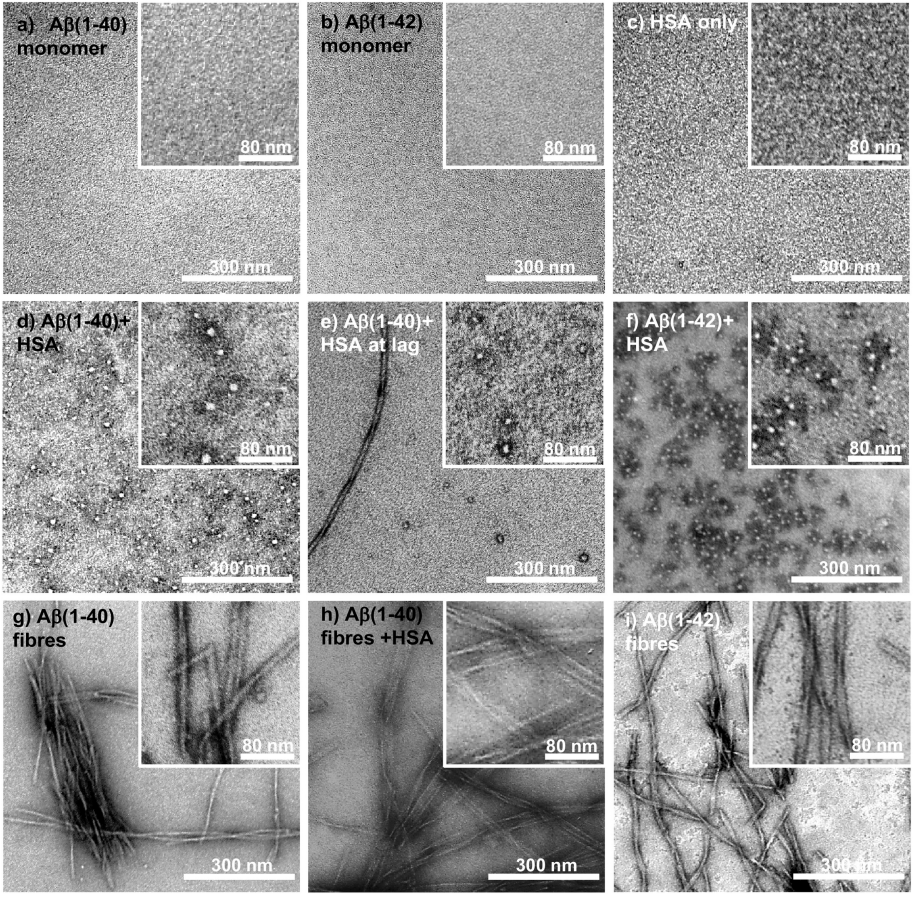
a) Aβ(1-40) monomer
80 nm
300 nm
b) Aβ(1-42) monomer
80 nm
300 nm
c) HSA only
80 nm
300 nm
d) Aβ(1-40)+ HSA
80 nm
300 nm
e) Aβ(1-40)+ HSA at lag
80 nm
300 nm
f) Aβ(1-42)+ HSA
80 nm
300 nm
g) Aβ(1-40) fibres
80 nm
300 nm
h) Aβ(1-40) fibres +HSA
80 nm
300 nm
i) Aβ(1-42) fibres
80 nm
300 nm

Figure 2

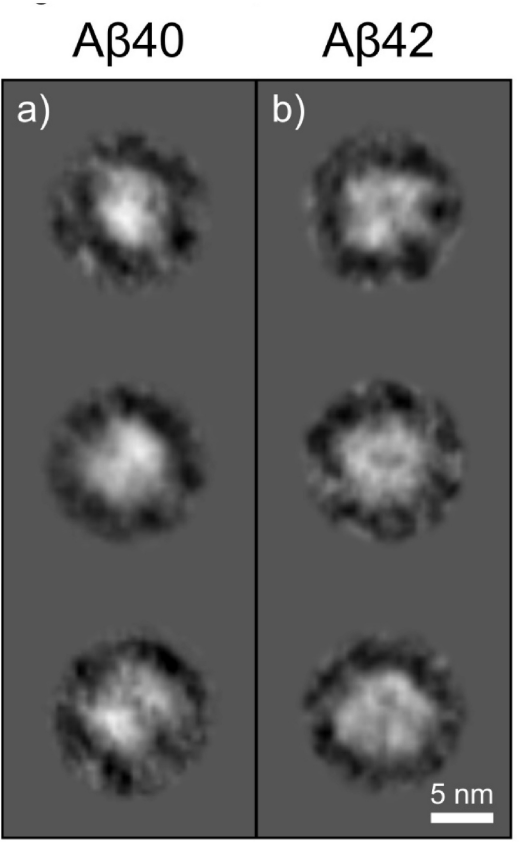

Figure 3

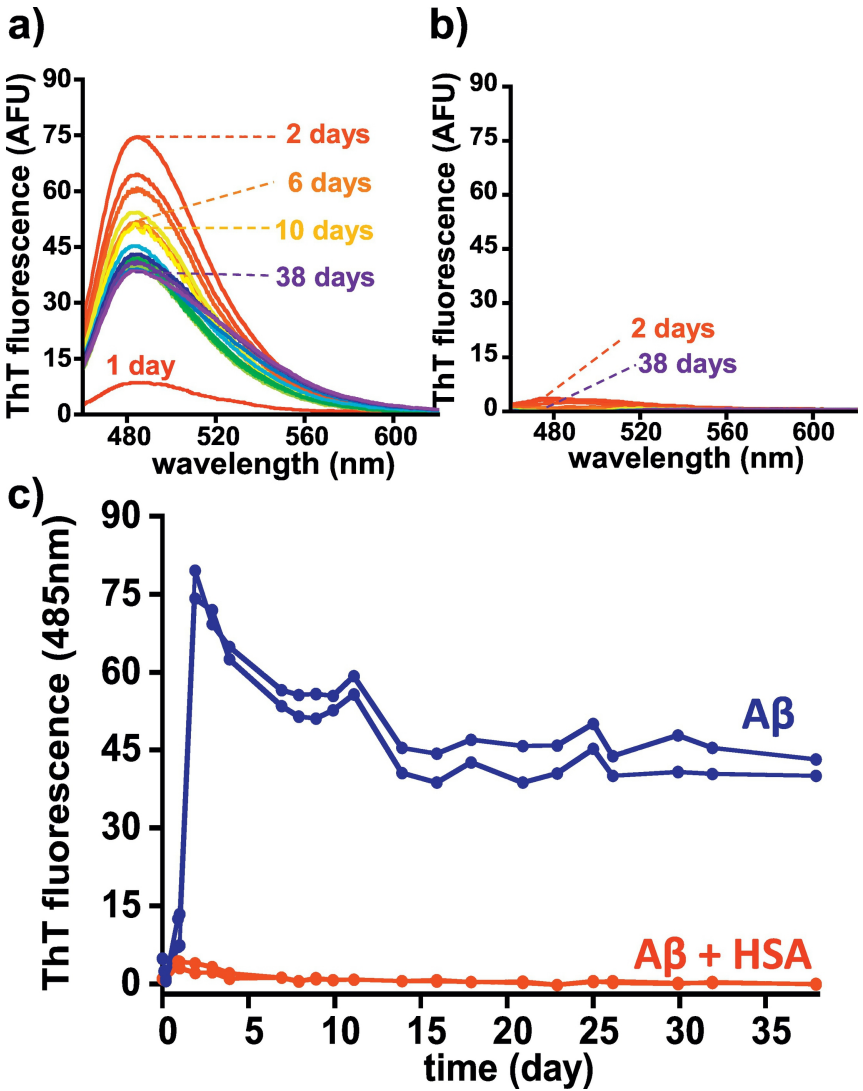
a)
ThT fluorescence (AFU)
90
75
60
45
30
15
0
480
520
560
600
wavelength (nm)
2 days
6 days
10 days
38 days
1 day
b)
ThT fluorescence (AFU)
90
75
60
45
30
15
0
480
520
560
600
wavelength (nm)
2 days
38 days
c)
ThT fluorescence (485nm)
90
75
60
45
30
15
0
0
5
10
15
20
25
30
35
time (day)
Aβ
Aβ + HSA

Figure 4

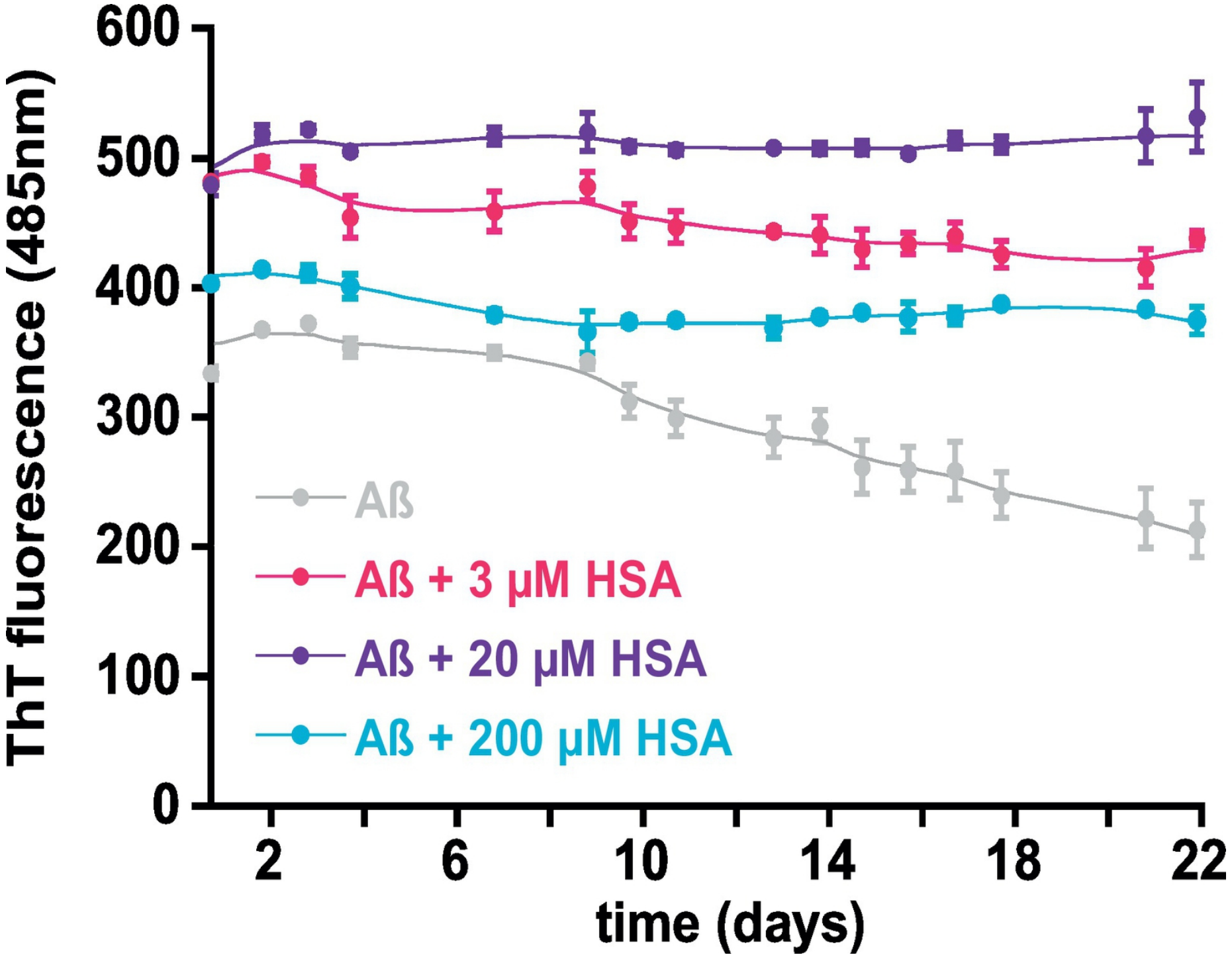
ThT fluorescence (485nm)
600
500
400
300
200
100
0
2
6
10
14
18
22
time (days)
Aß
Aß + 3 µM HSA
Aß + 20 µM HSA
Aß + 200 µM HSA

Figure 5

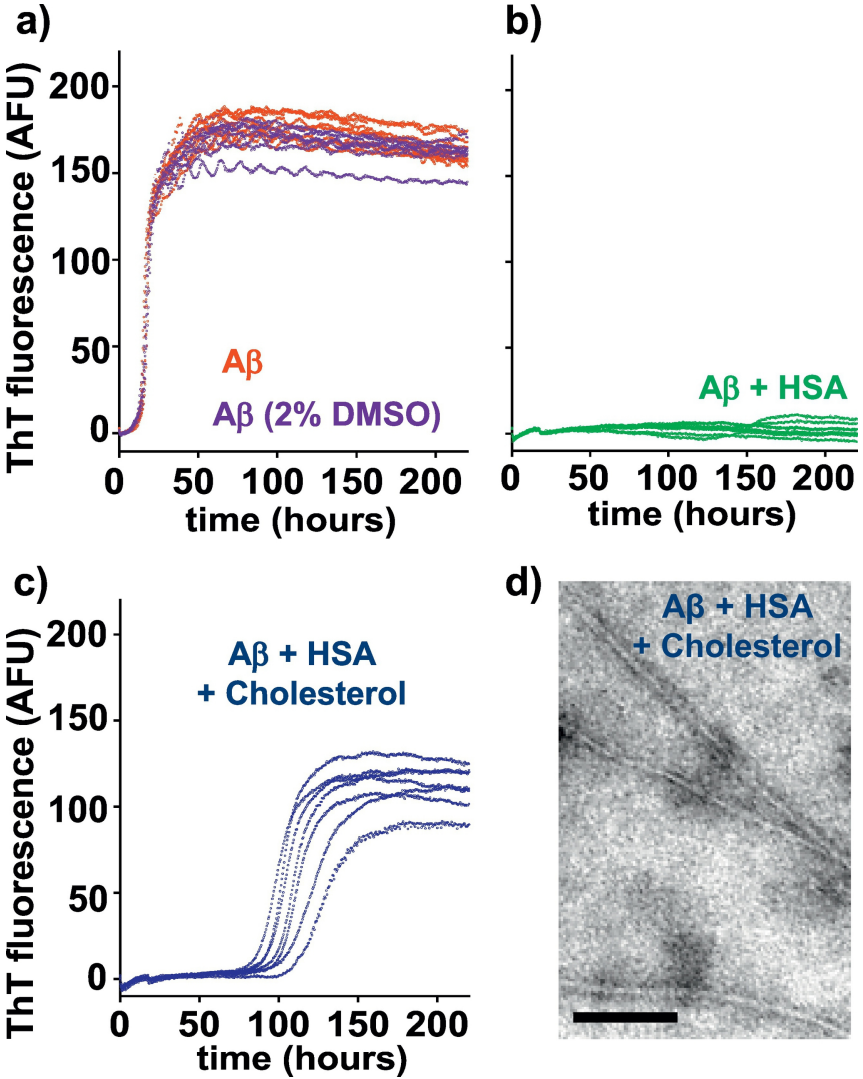
a)
ThT fluorescence (AFU)
200
150
100
50
0
Aβ
Aβ (2% DMSO)
0
50
100
150
200
time (hours)
b)
Aβ + HSA
0
50
100
150
200
time (hours)
c)
ThT fluorescence (AFU)
200
150
100
50
0
Aβ + HSA
+ Cholesterol
0
50
100
150
200
time (hours)
d)
Aβ + HSA
+ Cholesterol

Figure 6

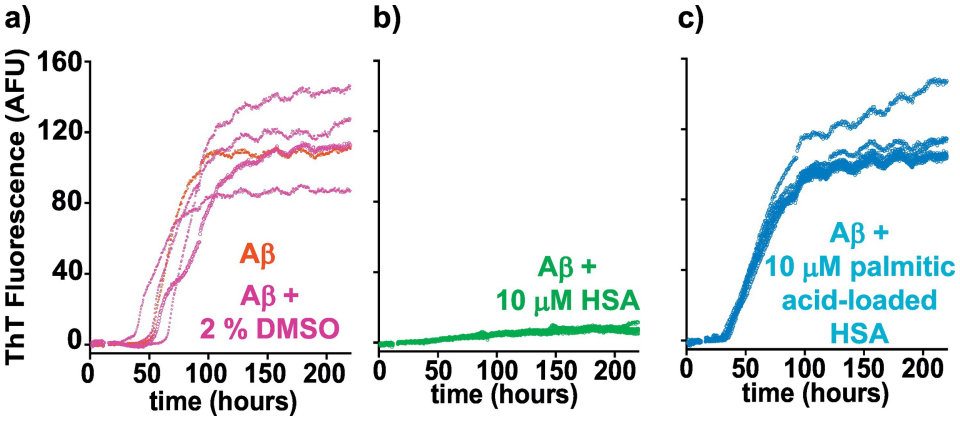
a)
b)
c)
ThT Fluorescence (AFU)
160
120
80
40
0
0
50
100
150
200
time (hours)
Aβ
Aβ +
2 % DMSO
Aβ +
10 μM HSA
Aβ +
10 μM palmitic
acid-loaded
HSA

Figure 7

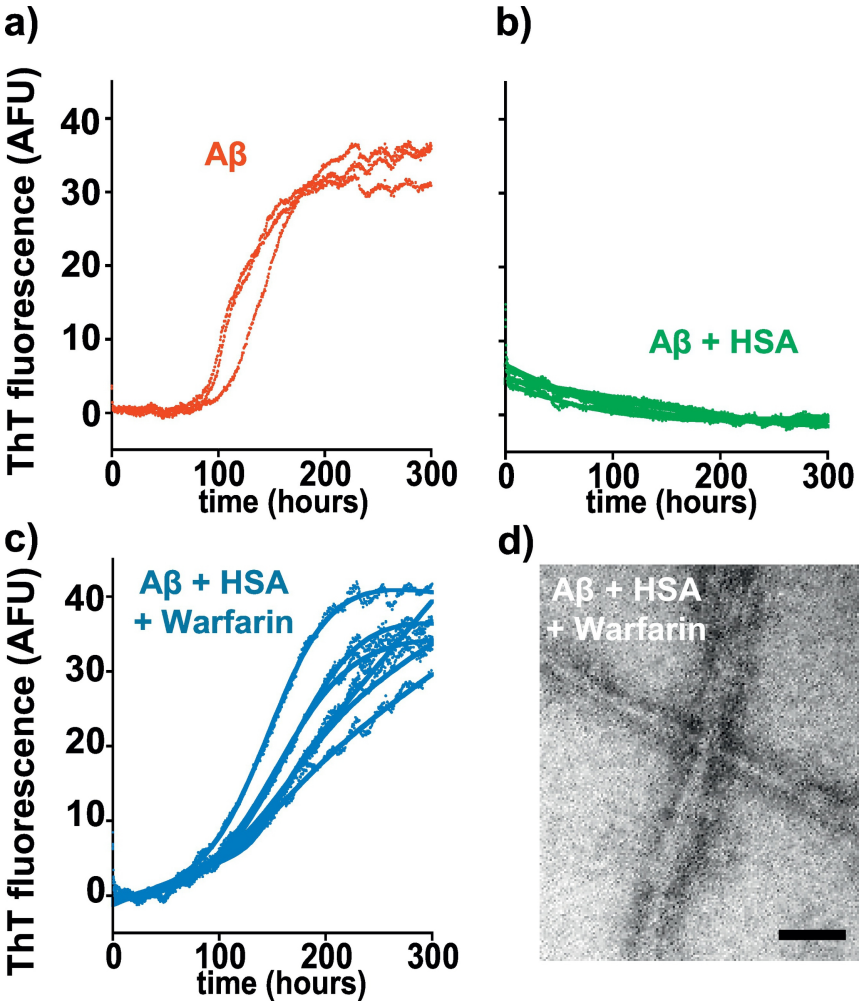
a)
ThT fluorescence (AFU)
40
30
20
10
0
Aβ
0
100
200
300
time (hours)
b)
Aβ + HSA
0
100
200
300
time (hours)
c)
ThT fluorescence (AFU)
40
30
20
10
0
Aβ + HSA
+ Warfarin
0
100
200
300
time (hours)
d)
Aβ + HSA
+ Warfarin

Figure 8

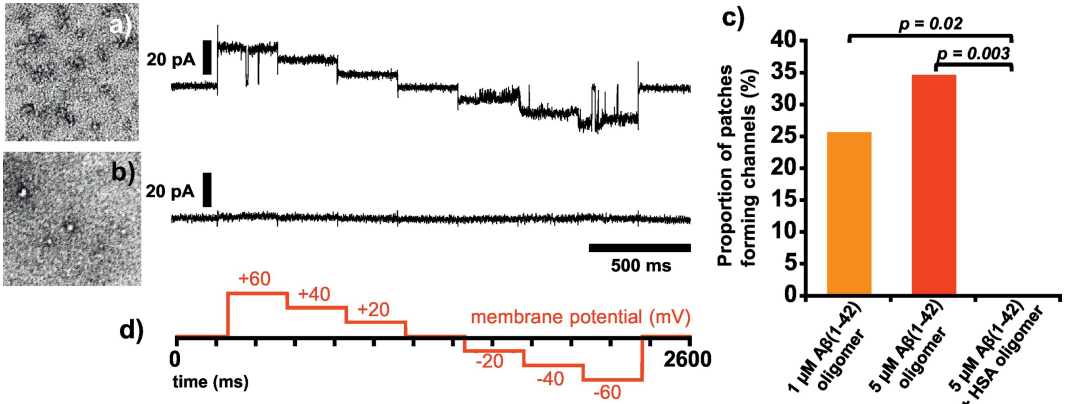
a)
20 pA
b)
20 pA
500 ms
d)
+60
+40
+20
membrane potential (mV)
0
time (ms)
2600
-20
-40
-60
c)
p = 0.02
p = 0.003
Proportion of patches forming channels (%)
40
35
30
25
20
15
10
5
0
1 µM Aβ(1-42) oligomer
5 µM Aβ(1-42) oligomer
5 µM Aβ(1-42) + HSA oligomer

Figure 9